successful in promoting formation of multicompartment cores (*32*).

References and Notes

1. M. Park, C. Harrison, P. M. Chaikin, R. A. Register, D. H. Adamson, *Science* **276**, 1401 (1997).
2. J. H. Collier, P. B. Messersmith, *Annu. Rev. Mater. Res.* **31**, 237 (2001).
3. R. Savic, L. Luo, A. Eisenberg, D. Maysinger, *Science* **300**, 615 (2003).
4. M. Shimomura, T. Sawadaishi, *Curr. Opin. Colloids Interface Sci.* **6**, 11 (2001).
5. I. W. Hamley, *The Physics of Block Copolymers* (Oxford Univ. Press, New York, 1998).
6. C. Park, J. Yoon, E. L. Thomas, *Polymer* **44**, 6725 (2003).
7. T. P. Lodge, *Macromol. Chem. Phys.* **204**, 265 (2003).
8. G. Riess, *Prog. Polymer Sci.* **28**, 1107 (2003).
9. A. Halperin, M. Tirrell, T. P. Lodge, *Adv. Polym. Sci.* **100**, 31 (1991).
10. A. Laschewsky, *Curr. Opin. Colloids Interface Sci.* **8**, 274 (2003).
11. E. T. Kisak, B. Coldren, C. A. Evans, C. Boyer, J. A. Zasadzinski, *Curr. Med. Chem.* **11**, 199 (2004).
12. D. E. Discher, A. Eisenberg, *Science* **297**, 967 (2002).
13. A. Kotzev, A. Laschewsky, P. Adriaensens, J. Gelan, *Macromolecules* **35**, 1091 (2002).
14. K. Stähler, J. Selb, F. Candau, *Langmuir* **15**, 7565 (1999).
15. R. Weberskirch, J. Preuschen, H. W. Spiess, O. Nuyken, *Macromol. Chem. Phys.* **201**, 995 (2000).
16. J.-F. Gohy, N. Willet, S. Varshney, J.-X. Zhang, R. Jérôme, *Angew. Chem. Int. Ed. Engl.* **40**, 3214 (2001).
17. Z. Zhou, Z. Li, Y. Ren, M. A. Hillmyer, T. P. Lodge, *J. Am. Chem. Soc.* **125**, 10182 (2003).
18. F. S. Bates, *Science* **251**, 898 (1991).
19. A. Balsamo *et al.*, *Macromolecules* **36**, 4515 (2003).
20. T. S. Bailey, C. M. Hardy, T. H. Epps, F. S. Bates, *Macromolecules* **35**, 7007 (2002).
21. T. Goldacker, V. Abetz, R. Stadler, I. Erukhimovich, L. Leibler, *Nature* **398**, 137 (1999).
22. N. Hadjichristidis, *J. Polym. Sci. Polym. Chem.* **37**, 857 (1999).
23. S. Sioula, N. Hadjichristidis, E. L. Thomas, *Macromolecules* **31**, 8429 (1998).
24. Z. Li, M. A. Hillmyer, T. P. Lodge, unpublished results.
25. Dynamic light scattering (DLS) data on dilute aqueous solutions of the μ-EOF samples were consistent with the cryo-TEM images. Namely, we typically observed a rather narrow distribution of relatively small micelles with hydrodyamic radii, in agreement with discrete micellar-like aggregates (Fig. 2), as well as a population of larger hydrodynamic particles consistent with the strings shown in Fig. 3. A description of the DLS technique and representative data (fig. S7) are given in (*26*).
26. Details of the cryo-TEM measurements and representative images of μ-EOF solutions with large fields of view are given on *Science* Online.
27. D. Danino, A. Bernheim-Groswasser, Y. Talmon, *Colloid Surf. A Physicochem. Eng.* **183**, 113 (2001).
28. E. E. Dormidontova, A. R. Khokhlov, *Macromolecules* **30**, 1890 (1997).
29. A. N. Semenov, I. A. Nyrkova, A. R. Khokhlov, *Macromolecules* **28**, 7491 (1995).
30. T. P. Lodge, M. A. Hillmyer, Z. Zhou, Y. Talmon, *Macromolecules* **37**, 6680 (2004).
31. S. Jain, F. S. Bates, *Science* **300**, 460 (2003).

32. This work was supported primarily by the Materials Research Science and Engineering Center program of NSF under award no. DMR-0212302.

Supporting Online Material

www.sciencemag.org/cgi/content/full/306/5693/98/DC1
Materials and Methods
Figs. S1 to S7
Table S1
References

28 July 2004; accepted 20 August 2004

Cope's Rule, Hypercarnivory, and Extinction in North American Canids

Blaire Van Valkenburgh,[1]* Xiaoming Wang,[2] John Damuth[3]

Over the past 50 million years, successive clades of large carnivorous mammals diversified and then declined to extinction. In most instances, the cause of the decline remains a puzzle. Here we argue that energetic constraints and pervasive selection for larger size (Cope's rule) in carnivores lead to dietary specialization (hypercarnivory) and increased vulnerability to extinction. In two major clades of extinct North American canids, the evolution of large size was associated with a dietary shift to hypercarnivory and a decline in species durations. Thus, selection for attributes that promoted individual success resulted in progressive evolutionary failure of their clades.

The history of large (>7 kg) predatory mammals is one of repeated ecological replacement (*1*). The various ecomorphological roles of cat-like, wolf-like, and hyena-like predator have been filled by representatives of distinct families at different times. In general, a single subfamily or family diversified and dominated a given ecomorphological role for about 10 million years and then declined, only to be replaced by a new clade. The expansion phase is often explained as a result of key adaptations and/or ecological opportunity, but it has been more difficult to understand the decline to extinction of a formerly successful group. Here we use the recently documented and exceptionally rich fossil record of North American canids (*2*, *3*) as a test case for studying the dynamics of extinction.

The dog family Canidae has three subfamilies: the extant Caninae, the extinct Hesperocyoninae [40 to 15 million years ago (Ma)], and the Borophaginae (34 to 2 Ma) (*4*). Both extinct subfamilies were endemic to North America and were very diverse in the Miocene, reaching a peak of 25 contemporaneous species approximately 30 Ma (Fig. 1A). The fossil record of these canids is impressive and well studied, with at least 28 species of hesperocyoninines and 68 species of borophagines described (*2*, *3*, *5*). In dental specialization and inferred diets, hesperocyonines ranged from relatively unspecialized mesocarnivores (inferred diet of small prey and plant matter) to more specialized hypercarnivores (inferred diet of large prey) characterized by enhanced shearing blades on their molar teeth (*2*). The more diverse borophagines included both of these types, as well as hypocarnivores (inferred diet of more plant matter than mesocarnivores) with reduced shearing blades and enlarged grinding areas on their molars (*3*).

To examine trends in body size and dietary specialization in fossil canids, we relied on inferences from dental morphology. Based on the established correlation between lower carnassial tooth [first molar (M_1)] length and body mass in living canids, we used M_1 length as a surrogate for body mass (*6*, *7*). To estimate dietary adaptations, we relied on previous studies of the correspondence between morphology and diet in canids (*8*, *9*). A discriminant analysis of 30 craniodental measurements on 27 species of modern canids easily separated hypercarnivores as having relatively deep jaws, large canine and incisor teeth, reduced molar grinding areas, and longer shearing blades on their lower carnassials (*9*). Because fossil species are rarely represented by complete specimens, we focused on three shape indices (six measurements) that together are highly informative about canid diets, independent of body mass. These are jaw depth relative to length, the proportion of the lower carnassial devoted to shearing rather than grinding function, and the proportion of the upper carnassial and molars devoted to grinding rather than shearing (*10*). Relative to hypo- and mesocarnivores, hypercarnivores tend to have deeper jaws to withstand loads imposed by killing and feeding on large prey, as well as long shearing blades and reduced molar grinding areas.

In both subfamilies, mean body mass increased substantially with time (Fig. 1, B and C) and within-lineage transitions to larger size significantly exceeded those to smaller

[1]Department of Ecology and Evolutionary Biology, University of California at Los Angeles, Los Angeles, CA 90095–1606, USA. [2]Department of Vertebrate Paleontology, Natural History Museum of Los Angeles County, 900 Exposition Boulevard, Los Angeles, CA 90007, USA. [3]Department of Ecology, Evolution, and Marine Biology, University of California at Santa Barbara, Santa Barbara, CA 93106, USA.

*To whom correspondence should be addressed. E-mail: bvanval@ucla.edu

size (*11*). In the Hesperocyoninae, M_1 length underwent a 400% expansion over 25 million years, and it increased by 600% over 35 million years in the Borophaginae. Increase in body size was accompanied by a disappearance of small species in both groups. The role of small canid-like carnivore was then filled by the earliest members of the Caninae (*3*), as well as perhaps a few species of procyonids (raccoon-like carnivores) (*12*).

A principal components analysis (PCA) of the three morphometric indices for 16 species of hesperocyonines for which the indices could be measured displays a diversity of forms and implies that the first principal component (PC1) can be used to infer hypercarnivorous adaptation (Table 1 and Fig. 2A). Species with the relatively deepest jaws, largest carnassial blades, and most reduced grinding areas have low, negative scores on this component, whereas those with less hypercarnivorous features have high positive scores. The second component further distinguishes species with deep jaws and reduced grinding area as having a very positive score on this axis. Within-lineage trends toward hypercarnivory are apparent within *Osbornodon* (N → P, Fig. 2A), as well as in the hypothesized lineage from *Mesocyon* to *Sunhunketanka* to *Enhydrocyon* (*2*) [H → G → (M and K), Fig. 2A].

The same analysis was run for 26 species of borophagines for which the three morphometric indices could be measured. Results largely parallel that for the hesperocyonines: PC1 defined an axis of hypercarnivory (Table 1 and Fig. 2A). Specialized hypercarnivores had low negative scores on this axis and positive scores on the second. As was true of the hesperocyonines, there were within-lineage trends toward hypercarnivory. For example, the proposed evolutionary sequence of *Paratomarctus* to *Carpocyon* to *Protepicyon* to *Epicyon* to *Borophagus* (*3*) can be traced across the PCA plot, moving from right to left on PC1 and then upward on PC2, as the lineage becomes increasingly specialized for hypercarnivory [s → v → (w and x) → y → z, Fig. 2A].

We used PC1 score as an index of specialization for hypercarnivory and plotted it against estimated body size for each species by subfamily. The pattern is unambiguous: Larger species are more specialized for hypercarnivory as defined by their position on PC1 (Fig. 2B). Moreover, there are no small species with adaptations for hypercarnivory as extreme as those seen in the larger species, nor are there large species with more mesocarnivorous or hypocarnivorous morphology. As mean body size increased, species evolved into specialized hypercarnivores.

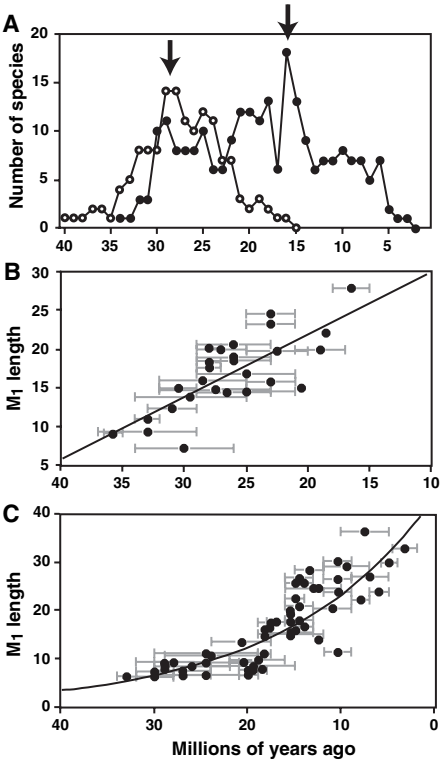

Fig. 1. Trends in species diversity and body size in extinct canids. (**A**) Changes in species diversity with time in hesperocyonines (open symbols) and borophagines (solid symbols). Arrows indicate the first appearance of species with hypercarnivorous adaptations as defined by a PCA of craniodental morphology. Body size (lower first molar length in millimeters) is plotted against time, from oldest to youngest, for species of (**B**) Hesperocyoninae ($n = 27$, $r^2 = 0.57$, $P < 0.001$) and (**C**) Borophaginae ($n = 60$, $r^2 = 0.74$, $P < 0.001$). Each bar spans the known species duration in the fossil record, with the symbol positioned at the midpoint. Diversity data are modified from (*2, 3*).

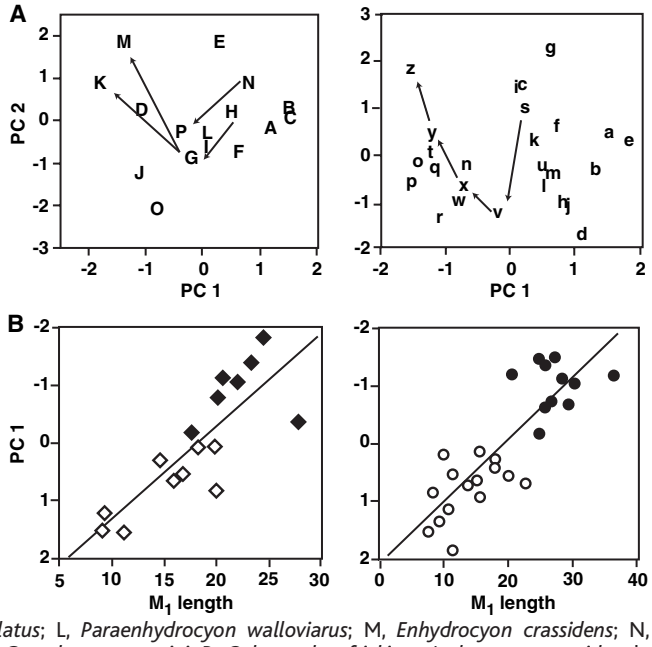

Fig. 2. Dietary specialization and its association with body size increase in hesperocyonines (left) and borophagines (right). (**A**) Plot of the first two PCs of a PCA of craniodental indices. Species with negative values on PC1 are predicted to have been hypercarnivorous to varying degrees. Arrows link species within a proposed evolutionary series. Species labels are as follows: A, *Hesperocyon gregarious*; B, *Prohesperocyon wilsoni*; C, *Hesperocyon coloradensis*; D, *Ectopocynus* sp.; E, *Paraenhydrocyon josephi*; F, *Cynodesmus thoides*; G, *Sunkahetanka geringensis*; H, *Mesocyon coryphaeus*; I, *Philotrox condoni*; J, *Enhydrocyon pahinsintewakpa*; K, *E. basilatus*; L, *Paraenhydrocyon walloviarus*; M, *Enhydrocyon crassidens*; N, *Osbornodon iamonensis*; O, *Cynodesmus martini*; P, *Osbornodon fricki*; a, *Archaeocyon pavidus*; b, *Rhizocyon oregonensis*; c, *Phlaocyon leucosteus*; d, *Cormocyon haydeni*; e, *C. copei*; f, *Desmocyon thomsoni*; g, *D. matthewi*; h, *Cynarctus galushai*; i, *Psalidocyon mariae*; j, *Microtomarctus conferta*; k, *Prototomarctus optatus*; l, *Tomarctus hippophagus*; m, *T. brevirostris*; n, *Aeleurodon aesthenostylus*; o, *A. mcgrewi*; p, *A. stirtoni*; q, *A. ferox*; r, *A. taxoides*; s, *Paratomarctus temerius*; t, *P. euthos*; u, *Carpocyon compressus*; v, *C. webbi*; w, *Protepicyon raki*; x, *Epicyon saveus*; y, *E. haydeni*; z, *Borophagus secundus*. (**B**) Degree of hypercarnivorous specialization (PC1 score in PCA analysis) plotted against body size (M_1 length in millimeters) (hesperyocyonines, $n = 16$, $r^2 = 0.67$, $P < 0.001$; borophagines, $n = 26$, $r^2 = 0.71$, $P < 0.001$). Note that values on PC1 are reversed. Putative hypercarnivores with PC1 score < 0 are indicated by solid symbols; hypo- and mesocarnivores (PC1 > 0) are indicated by open symbols. For analyses of body size trends, all species in (*2*, *3*) for which lower first molar length was available were included.

Table 1. Variable loadings and variance explained for the first two PCs.

	Hesperocyoninae		Borophaginae	
Variables	PC1	PC2	PC1	PC2
Relative blade length	–0.947	–0.171	–0.929	–0.247
Relative grinding area	0.812	–0.581	0.936	0.186
Relative jaw depth	–0.911	–0.34	–0.891	0.453
Percent variance explained	80%	16%	84.5%	10%

Did this result in an increased susceptibility to extinction? A plot of the index of hypercarnivory (PC1 score) against estimated species durations (Fig. 3A) indicates that none of the hypercarnivorous species (solid symbols) persisted for more than six million years, whereas some more omnivorous species (open symbols) endured for as much as 11 million years. Thus, the large hypercarnivores appear to have been limited in duration relative to other species, suggesting a greater vulnerability to extinction.

The shorter species longevities of large hypercarnivores might reflect a decreased probability of fossil preservation. Because they were large and carnivorous, their population densities are expected to have been reduced relative to those of smaller species (*13*–*15*), making them less likely to be recovered as fossils. Conversely, their greater body size, more massive bones and teeth, and presumed large geographic ranges favor fossil preservation (*16*, *17*). The mean frequency of borophagine species in individual fossil localities (194 occurrences) is approximately 0.02, and that of hesperocyonines (39 occurrences) is approximately 0.03 (*18*). Relative abundance in a fossil sample is uncorrelated with observed species duration or body size in both subfamilies (Fig. 3B). Based on these observed frequencies and calculating binomial probabilities (*19*), it would require a total fossil sample of 500 to 2000 specimens to be 99% or more certain of recovering at least one specimen of each canid species, if present. Thus, we can regard the observed endpoints of species ranges as being accurate indicators of the true stratigraphic ranges when samples approach or exceed these sizes for the interval above and below a given observed endpoint interval. At the temporal resolution we used, the known fossil record is sufficiently rich in each of the major regions that this condition is easily met at most levels throughout the Oligocene and Miocene. Given this, we do not believe that the observed differences in species durations result from artifacts of sampling.

Because hypercarnivory and increased body size evolved in tandem within our sampled canids, it is unclear which is most responsible for the drop in species durations. Both are associated with reduced population densities, a pivotal factor in modern species extinctions (*20*). Examination of the histories of each subfamily reveals that the first appearance of hypercarnivores (here defined as PC1 score < 0) occurs at the diversity peak in each subfamily (Fig. 1A). Subsequently, each subfamily declines to extinction over the next 14 to 16 million years. In both, new species continue to appear after the diversity peak, but extinction outpaces origination and species durations are shortened, leading to progressive declines in species richness.

Cope's rule, or the evolutionary trend toward larger body size, is common among mammals (*21*). Large size enhances the ability to avoid predators and capture prey, enhances reproductive success, and improves thermal efficiency (*22*, *23*). Moreover, in large carnivores, interspecific competition for food tends to be relatively intense, and bigger species tend to dominate and kill smaller competitors (*24*, *25*). Progenitors of hypercarnivorous lineages may have started as relatively small-bodied scavengers of large carcasses, similar to foxes and coyotes, with selection favoring both larger size and enhanced craniodental adaptations for meat eating. Moreover, the evolution of predator size is likely to be influenced by changes in prey size, and a significant trend toward larger size has been documented for large North American mammals, including both herbivores and carnivores, in the Cenozoic (*21*). After 30 Ma, large (>100 kg) prey species were always present and tended over time to become an increasingly significant resource (*26*).

Among living meat eaters, almost all species larger than about 21 kg prey on species as large or larger than themselves, whereas smaller carnivores can subsist on much smaller prey (such as invertebrates and rodents) (*27*). This transition to taking larger prey seems to reflect energetic constraints imposed by tradeoffs between foraging effort and food acquired. For species > ~21 kg, energy spent acquiring small prey is not likely to be balanced by nutrition gained (*27*). Thus, as moderately carnivorous hesperocyonines and borophagines became larger, they crossed the threshold where taking big prey was favored. Based on the relation between M_1 length and body mass in living canids (*6*, *7*), this threshold would have been crossed at an M_1 length of 18 to 25 mm. In both subfamilies, this transition was coincident with the first appearance of species with negative PC1 scores (Fig. 2B), which our analysis suggests were hypercarnivores. To be an effective predator of large prey required additional morphological specializations such as deeper jaws, reduced dental grinding areas, and enlarged dental shearing blades. Once species reached this elevated position in the trophic chain, their vulnerability to extinction increased. Reversals to a more generalized morphology and diet were rare in these two extinct canid subfamilies (*2*, *3*). Consequently, selection for larger size and hypercarnivory acted as a macroevolutionary ratchet, locking them into a trend of increasingly specialized forms that resulted ultimately in clade extinction. Similar trends toward larger size and hypercarnivory have been suggested in other extinct predatory taxa, such as Permian therapsids (*28*), creodonts, amphicyonids, and hyaenids (*1*), and these clades may have succumbed to the same macroevolutionary ratchet. Evolution may progress in a direction that favors individual fitness but ultimately

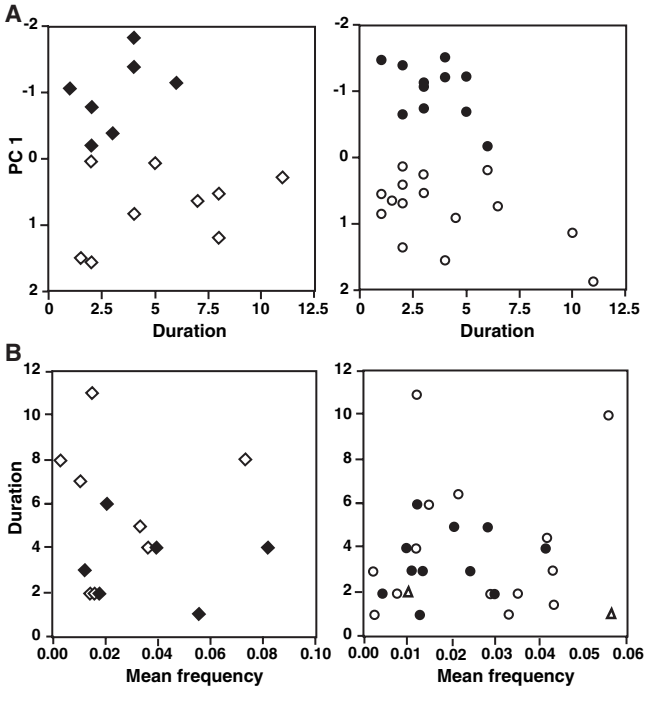

Fig. 3. Dietary specialization, species duration, and frequency in collections in hesperocyonines (left) and borophagines (right). Solid symbols, putative hypercarnivores with PC1 score < 0; open symbols, hypo- and mesocarnivores (PC1 > 0); open triangles, species not included in PC analysis because of insufficient data. Species durations were determined from published data (*2*, *3*) on stratigraphic range and are minima, given that the fossil record is unlikely to preserve either the first or last representative of a species. (**A**) PC1 score plotted against species durations (hesperocyonines, $n = 16$, $r^2 = 0.03$, $P = 0.55$; borophagines, $n = 26$, $r^2 = 0.1$, $P = 0.12$). Note that values on PC1 are reversed. (**B**) Species durations plotted against mean frequency in individual fossil collections. (hesperocyonines, $n = 14$, $r^2 = 0.01$; $P = 0.73$; borophagines, $n = 27$, $r^2 = 0.004$, $P = 0.74$). M_1 length is also not correlated with mean frequency (analysis not shown; hesperocyonines, $n = 14$, $r^2 = 0.004$; $P = 0.82$; borophagines, $n = 26$, $r^2 = 0.007$, $P = 0.69$).

results in a lineage that is less likely to persist (*29*). The risk of extinction will rise if the evolutionary trend is associated with a decline in population density and/or increased trophic specialization (given that reversals are uncommon). The same or a similar ratchet might be responsible for the decline to extinction of many formerly successful groups of organisms, especially in mammals, where Cope's rule is often observed and species turnover rates tend to be high (*21*, *29*).

References and Notes

1. B. Van Valkenburgh, *Annu. Rev. Earth Planet. Sci.* **27**, 463 (1999).
2. X. Wang, *Bull. Am. Mus. Nat. Hist.* **221**, 1 (1994).
3. X. Wang, R. H. Tedford, B. Taylor, *Bull. Am. Mus. Nat. Hist.* **243**, 1 (1999).
4. R. H. Tedford, in *Nutrition and Management of Dogs and Cats* (Ralston Purina, St. Louis, MO, 1978), chap. M23.
5. B. Van Valkenburgh, T. Sacco, X. Wang, *Bull. Am. Mus. Nat. Hist.* **278**, 147 (2003).
6. B. Van Valkenburgh, in *Body Size in Mammalian Paleobiology*, J. Damuth, B. MacFadden, Eds. (Cambridge Univ. Press, Cambridge, 1990), pp. 181–205.
7. To predict the body mass of the extinct canids, we used the allometric relation established for living canid species [$\log_{10}$ $Mass_{kg}$ = 1.82($\log_{10}$ $M_1Length_{mm}$) – 1.22; n = 27, r = 0.87]. Using this equation, the smallest hesperocyonine in our sample weighed about 2 kg and the largest 26 kg. The same values for the borophaginae are 2 kg and 42 kg.
8. B. Van Valkenburgh, *Paleobiology* **17**, 340 (1991).
9. B. Van Valkenburgh, K. Koepfli, *Symp. Zool. Soc. London* **65**, 15 (1993).
10. These measurements are as follows: jaw length, distance between posterior margin of mandibular condyle and anterior margin of canine tooth; jaw depth, maximum dorsoventral depth of dentary measured at junction of M_1 and M_2; lower carnassial length, maximum mesiodistal length of lower M_1; lower carnassial blade length, maximum mesiodistal length of the M_1 trigonid; upper carnassial length, maximum mesiodistal length of upper fourth premolar; upper molar grinding area, the sum of the products of width and length of upper M^1 and M^2. Morphometric indices are as follows: relative jaw depth = jaw depth/jaw length; relative blade length = lower M_1 trigonid length/lower M_1 length; relative grinding area = square root of upper molar grinding area/upper carnassial length. All measurements were made with calipers by X.W.
11. Current researchers often define Cope's rule as a net tendency toward size increase throughout a clade's entire history and across all of its lineages (*21*, *30*). Our conclusions do not depend on the satisfaction of this strict definition, only on whether canid clades were dominated by species of large body size and hypercarnivorous diets relatively late in their histories. Nevertheless, based on the sample of phylogenetically independent ancestor/descendant size transitions implied by the full phylogenies for each clade (*2*, *3*), in both subfamilies, numbers and magnitudes of size increases significantly exceeded size decreases [hesperocyonines, 11+, 2–, P = 0.02 (sign test), P = 0.01 (Wilcoxon signed rank test); borophagines, 16+, 6–, P = 0.05 (sign test), P = 0.04 (Wilcoxon signed rank test); species sizes are based on the average length of the first lower molar; Wilcoxon tests are based on log (base 10)–transformed data].
12. J. A. Baskin, in *Evolution of Tertiary Mammals of North America*, C. M. Janis, K. M. Scott, L. L. Jacobs, Eds. (Cambridge Univ. Press, Cambridge, 1998), pp. 144–151.
13. J. Damuth, *Nature* **290**, 699 (1981).
14. J. Damuth, *Biol. J. Linn. Soc* **31**, 193 (1987).
15. J. Damuth, *Nature* **365**, 748 (1993).
16. A. K. Behrensmeyer, D. Western, D. E. Dechant Boaz, *Paleobiology* **5**, 12 (1979).
17. J. Damuth, *Paleobiology* **8**, 434 (1982).
18. The mean frequency of each canid species in individual fossil collections where it occurs was based on the number of canid specimens reported, by locality (*3*, *4*), for those species used in the PCA. These values were divided by the total number of specimens collected from the respective localities, when available. Only collections totaling ≥15 specimens were used. Sources for total specimen numbers included some literature compilations (*31*, *32*), direct counts of museum specimens, and numbers of specimens reported in online museum catalogs (Univ. of California Museum of Paleontology, Berkeley, CA; Field Museum of Natural History, Chicago, IL; American Museum of Natural History, New York; Yale Peabody Museum, New Haven, CT). The catalog sources likely sometimes inflate the canid frequencies by not including uncataloged material, but in cases where comparisons could be made, the values derived from the three sources were in rough agreement. The mean for each species is based on from 1 to 24 collections (average, 5.3) and represents a total of 233 species occurrences.
19. J. C. Barry *et al.*, *Paleobiology* **28** (suppl.), 1 (2002).
20. A. Purvis, J. L. Gittleman, G. Cowlishaw, G. M. Mace, *Proc. R. Soc. London Ser. B* **267**, 1947 (2000).
21. J. Alroy, *Science* **280**, 731 (1998).
22. M. L. McKinney, in *Evolutionary Trends*, K. J. McNamara, Ed. (Univ. of Arizona Press, Tucson, AZ, 1990), pp. 75–120.
23. S. Stanley, *Evolution* **27**, 1 (1973).
24. F. Palomares, T. M. Caro, *Am. Nat.* **153**, 492 (1999).
25. B. Van Valkenburgh, in *Meat-Eating and Human Evolution*, C. Stanford, H. T. Bunn, Eds. (Oxford Univ. Press, Oxford, 2001), pp. 101–121.
26. C. M. Janis, K. M. Scott, L. L. Jacobs, Eds., *Evolution of Tertiary Mammals of North America* (Cambridge Univ. Press, Cambridge, 1998).
27. C. Carbone, G. M. Mace, S. C. Roberts, D. W. Macdonald, *Nature* **402**, 286 (1999).
28. B. Van Valkenburgh, I. Jenkins, in *The Fossil Record of Predation*, M. Kowalewski, P. H. Kelley, Eds. (The Paleontological Society Papers, The Paleontological Society, Washington, DC, 2002), vol. 8, pp. 267–288.
29. S. Stanley, *Macroevolution: Pattern and Process*. (Freeman, San Francisco, CA, 1979).
30. D. Jablonski, *Nature* **385**, 250 (1997).
31. M. F. Skinner, F. W. Johnson, *Bull. Am. Mus. Nat. Hist.* **178**, 215 (1984).
32. M. R. Voorhies, "Vertebrate paleontology of the proposed Norden Reservoir area, Brown, Cherry, and Keya Paha Counties, Nebraska: Lincoln, Nebraska" (Technical Report 82-09, Univ. of Nebraska, prepared for the U.S. Bureau of Reclamation, 1990).

33. For helpful comments on the manuscript, we thank P. Adam, A. R. Friscia, J. Meachan, J. Samuels, R. H. Tedford, R. K. Wayne, M. Webster, participants in the UCLA Paleobiology journal club, and two anonymous reviewers.

7 July 2004; accepted 26 August 2004

Basis for Structural Diversity in Homologous RNAs

Andrey S. Krasilnikov,[1] Yinghua Xiao,[1] Tao Pan,[2] Alfonso Mondragón[1]*

Large RNA molecules, such as ribozymes, fold with well-defined tertiary structures that are important for their activity. There are many instances of ribozymes with identical function but differences in their secondary structures, suggesting alternative tertiary folds. Here, we report a crystal structure of the 161-nucleotide specificity domain of an A-type ribonuclease P that differs in secondary and tertiary structure from the specificity domain of a B-type molecule. Despite the differences, the cores of the domains have similar three-dimensional structure. Remarkably, the similar geometry of the cores is stabilized by a different set of interactions involving distinct auxiliary elements.

Ribonuclease (RNase) P is one of only two known ribozymes conserved in all taxonomic kingdoms and is responsible for maturation of the 5′ end of tRNA (*1*, *2*). It is a multiple-turnover endonuclease that contains an RNA subunit and protein components. In bacteria, the RNA subunit is capable of cleaving pre-tRNA without its protein partner in vitro (*3*, *4*). Most of the bacterial RNase Ps can be classified into two major distinct types—A and B—on the basis of the sequence of the RNA component. In both types of bacterial RNase P, the RNA consists of two independently folding domains: a specificity domain and a catalytic domain. The specificity (S) domain is responsible for substrate recognition and binding (*5*, *6*).

Although the RNA components of all bacterial RNase P types share many secondary-structural features throughout the molecule, there are noticeable differences (*3*, *4*). In particular, the S domains of the two major bacterial types exhibit differences in secondary structure that might affect the tertiary fold (Fig. 1). Most noticeably, in the A-type RNase P, the P10.1 stem is absent and the J12/11 internal loop is interrupted by the insertion of the P13 and P14 stems, which are not present in the B type. Because the major tertiary interactions in the S domain of B-type RNase P involve the P10.1 stem (*7*), a substantially different fold for the A-type RNase P could be anticipated. However, biochemical data indicate that substrate recognition involves equivalent nucleotides in both types (*8*, *9*), suggesting similar structures for the pre-tRNA recognition region.

[1]Department of Biochemistry, Molecular Biology, and Cell Biology, Northwestern University, Evanston, IL 60208, USA. [2]Department of Biochemistry and Molecular Biology, University of Chicago, 920 East 58th Street, Chicago, IL 60637, USA.

*To whom correspondence should be addressed. E-mail: a-mondragon@northwestern.edu